BNL - 66940

High Resolution Microtomography for Density and Spatial Information about Wood Structures

Barbara Illman
USDA/FS Forest Products Laboratory
University of Wisconsin
Madison, WI 53705

Betsy Dowd
National Synchrotron Light Source
Brookhaven National Laboratory
Upton, NY 11973

July 1999

National Synchrotron Light Source

Brookhaven National Laboratory
Operated by
Brookhaven Science Associates
Upton, NY 11973

Under Contract with the United States Department of Energy
Contract Number DE-AC02-98CH10886

DISCLAIMER

High Resolution Microtomography for Density and Spatial Information about Wood Structures

Barbara Illman[1a] and Betsy Dowd[b]
[a]USDA/FS Forest Products Laboratory, University of Wisconsin, Madison, WI 53705
[b]National Synchrotron Light Source, Brookhaven National Laboratory, Upton, NY 11193

ABSTRACT

Microtomography has successfully been used to characterize loss of structural integrity of wood. Tomographic images were generated with the newly developed third generation x-ray computed microtomography (XCMT) instrument at the X27A beamline at the national Synchrotron Light source (NSLS). The beamline is equipped with high-flux x-ray monochromator based on multilayer optics developed for this application. The sample is mounted on a translation stage with which to center the sample rotation, a rotation stage to perform the rotation during data collection and a motorized goniometer head for small alignment motions. The absorption image is recorded by a single-crystal scintillator, an optical microscope and a cooled CCD array detector. Data reconstruction has provided three-dimensional geometry of the heterogeneous wood matrix in microtomographic images. Wood is a heterogeneous material composed of long lignocellulose vessels. Although wood is a strong natural product, fungi have evolved chemical systems that weaken the strength properties of wood by degrading structural vessels. Tomographic images with a resolution of three microns were obtained nonintrusively to characterize the compromised structural integrity of wood. Computational tools developed by Lindquist et al (1996) applied to characterize the microstructure of the tomographic volumes.

Keywords: microtomography, synchrotron x-ray tomography, wood

1. INTRODUCTION

Synchrotron X-ray computed microtomography (XCMT) was used to characterize structures in sound wood and loss of this structural integrity caused by fungal degradation. The data was acquired with the third-generation XCMT instrument located at the X27A beamline of the National Synchrotron Light Source[2]. X-ray computed tomography provides volumetric data of element composition nondestructively, by mapping the three-dimensional X-ray absorption through the sample.

Wood is a renewable natural resource that has remarkably high strength per unit weight, making it an ideal structural material. Loss of structural integrity from degradation by brown-rot wood decay fungi results in strength loss and failure of wood in service. Strength loss can occur early in the decay process. Information is needed about the early stages of decay in order to design environmentally compatible prevention and control measures[1]. Wood strength is due to xylem tissue that is composed of cellulose, lignin and hemicellulose. The xylem of pine wood contains elongated, vertical cells called tracheids that account for approximately 90% of pine wood biomass. Tracheids are thick-walled, tubular structures that have hollow centers or pores containing air and/or water. The tracheid pore, anatomically referred to as the cell lumen, is a major port of entry for decay fungi. Fungal enzymes and metabolites degrade cell walls of tracheids[6], as evidenced by wall erosion and microscopic breaks in the walls. The biochemical mechanisms of wood decay fungi are not clearly understood[8]. The objective of this study was to characterize structure and matrix changes of wood during incipient decay using high-resolution tomography and computational tools to analyze structural geometry in tomographic images.

Using XCMT, density differences between diverse chemical structures can be recorded in reconstructed images of a heterogeneous matrix such as wood. The density differences between layers of cell walls, between walls and zones surrounding contiguous cells were measured. Consequently, XCMT can be readily applied to the analysis of spatial

[1]Correspondence: Email: billman@facstaff.wisc.edu
WWW: http://www.fpl.fs.fed.us/program/htm
Telephone: 608 231 9231; Fax: 608-231-9262

distribution and interconnectivity of a pore through a volume of material. In this experiment, density differences between tracheal walls and pore cavity were observed in the reconstructed images of control non-degraded wood and in wood exposed to the fungus. Breakdown in the regular structure of cell walls was apparent in the tomographic slices reconstructed from the samples exposed to the fungus. The degree and direction of wall erosion was determined by analyzing the segmented data with a 3-dimensional medial axis analysis program (3DMA) developed by Brent Lindquist and colleagues at the State University of New York at Stony Brook[10]. Volumetric data such as porosity, pore size and distribution interconnectivity of pores was calculated for each sample.

2. EXPERIMENTAL DESIGN

2.1 Sample preparation

Wood specimen and fungal cultures were prepared at the USDA Forest Service, Forest Products Laboratory, a facility maintained in conjunction with the University of Wisconsin, Madison, WI. Southern yellow pine wood blocks taken from a 2 in x 4 in x 4 ft piece of lumber were cut into (approximately 1.5 mm x 1.5 mm x 10 cm) morphologically uniform spring-wood specimen for XCMT analysis. Specimen were sterilized by autoclave and stored in sterile containers. The brown-rot wood decay fungus, *Gloeophyllum trabeum*, was obtained from the culture collection at the Forest Products Laboratory. The fungus was inoculated onto 2% malt extract agar (MEA) medium in petri dishes and allowed to grow in the dark at 27 °C, 70% relative humidity for two weeks. Wood and fungal specimen were transported to and stored at NSLS under sterile conditions. Prior to XCMT analysis, four pieces of wood were inoculated with *G. trabeum* by placing the specimen on fungal mycelia in a petri dish. Cultures were stored in the dark in a closed container to prevent dehydration.

2.2 XCMT Instrument and Data Collection

The synchrotron radiation is filtered by a monochromator comprised of a highly efficient pair of W-B_4C multilayers deposited on Silicon substrates. Energy tunability is from 5 to 13 keV, with a $\Delta E/E$ of about 1.5%. The XCMT workstation incorporates a cooled charge-coupled device (CCD) with 1317 x 1035 pixels; the CCD can record the data to reconstruct up to 1035 horizontal slices, simultaneously[2]. During XCMT data acquisition, the shadow of the test sample formed on the surface of a YAG:Ce crystal is imaged with a microscope objective, onto a Photometrics PXL-1400 CCD camera. (Figure 1). The magnified image of the shadow, a 2-D linear X-ray attenuation map of the sample, is digitally recorded by the CCD camera at regular angular intervals, producing angle-dependent views of the attenuation map as the sample is rotated over a full 180 degrees.

To prevent aliasing in the reconstruction, the number of recorded views of the sample must be greater than or equal to the column number of CCD pixels, N, multiplied by $\pi/2$[4,9]. These $N\pi/2$ views are then processed using a Fourier-based Fast Filtered Back Transform algorithm to generate M transverse images or slices through the sample for every row of the CCD. These reconstructed slices are then stacked to produce a MxNxN volume representation of the sample.

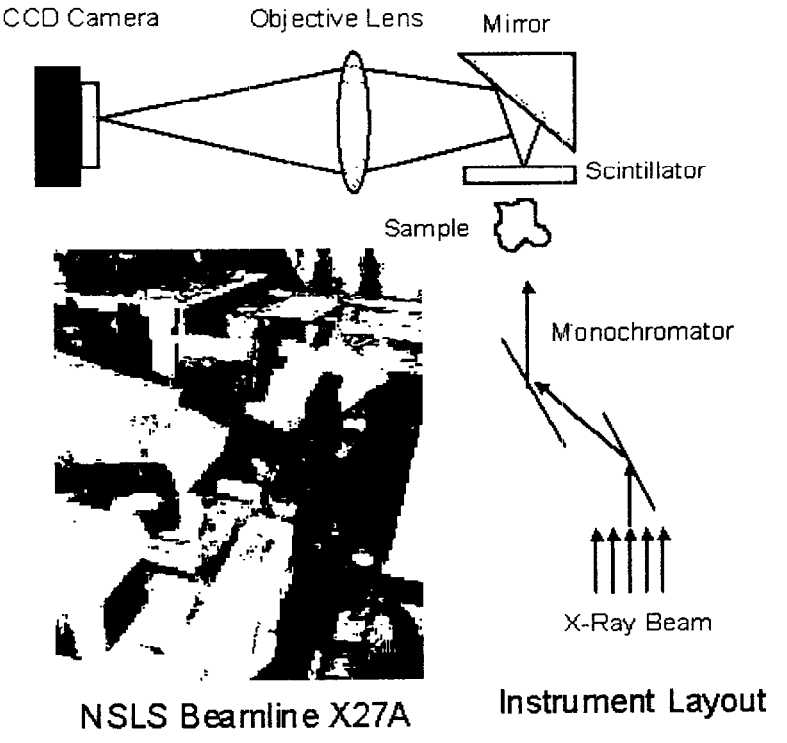

Figure 1. XCMT apparatus

All measurements were performed with the monochromator tuned above the Copper k-edge, at about 9 keV. Over the 4-day fungus test, each wood sample was imaged onto the CCD using a Nikon 5x achromatic objective. The 6.8-micron square pixels were binned, or electronically summed, by a factor of 4x in both x and y, resulting in improved signal to noise ratio. Five hundred views of a 1.8 mm x 1.4 mm sample area were acquired at angular intervals of .36 degrees in order to generate microtomographic data for accurate reconstruction. The resultant digitized volume contained 28 million voxels of size 5-microns-cubed.

Non-inoculated control and inoculated test specimens of wood were scanned for tomographic acquisition at 24, 42, 68 and 92 hours after fungal inoculation. For XCMT scans, a wood specimen was mounted with tracheids in a vertical position on a motorized x-y stage for centering the sample in the optical field of view. The sample stage in turn is mounted to the rotational stage used to perform data collection. This entire assembly mounts to the tilt and translational stages necessary for accurate prealignment of the rotational stage to the CDD. The non-inoculated control sample was scanned at the beginning and at the end of the experiment. Between scans, the control was stored in sterile conditions. At each time period, an inoculated specimen was removed from culture, scanned and discarded.

3. DATA ANALYSIS

3.1 Data Reconstruction and Rendering

The collected raw data files were saved to disk for subsequent processing. A Fast Filtered Back Transform (FFBT), developed at Brookhaven National Laboratory was used to reconstruct the slices from the raw data[2,11]. A volume of the reconstructed slices was rendered for each set of sample data collected. The value of each voxel in the volume represents the linear attenuation coefficient over the pixel area. Gray or color scale images of the reconstructed data, therefore, can provide great insight into the composition of a material. A volume of control wood was reconstructed using Fortner Software's T3D (Figure 2).

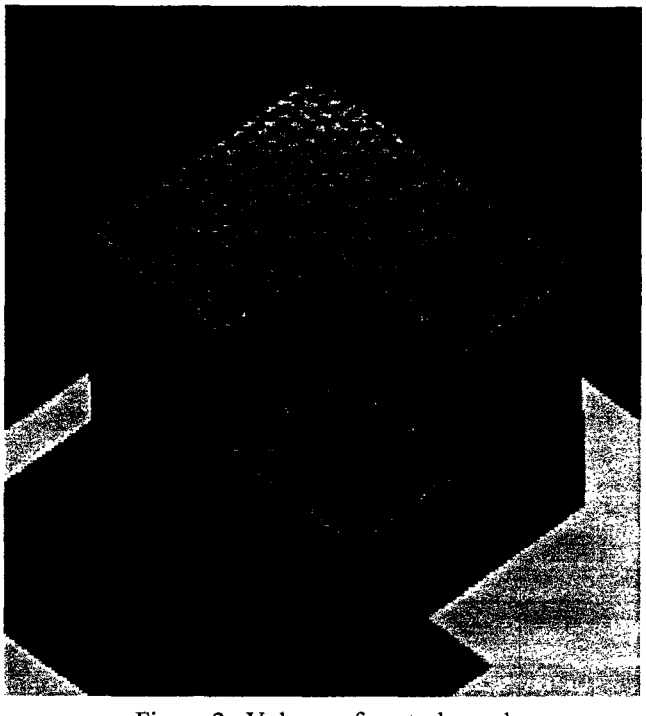

Figure 2. Volume of control wood

In addition to differences within the tracheids, we are interested in clearly defining the edges of the wood matrix and monitoring breakdown of the cell walls during exposure to fungus. It was assumed that the fungus would be largely transparent due to its low attenuation coefficient and segmented as air. The damage incurred by the wood due to the traversal of the fungus would appear therefore as an increase in irregular wood structure accompanied by an increase of pore space in the location of the fungus. To perform the analysis, wall must be discriminated from pore, ignoring any density differences within the wall. In other words, gray scale images need to be converted to simple black and white images by identifying each voxel with an attenuation coefficient greater than some cutoff value as solid (wood), and those below the threshold as air or pore. Structures in Figure 2 with the highest density are reddish-brown, medium density are brown and lowest density are blue. Ray cells are reddish-brown, tracheid cell walls are brown and pores are blue. The middle lamella, spaces between tracheids, have the highest density with dark reddish-brown color. Middle lamella are known to contain high concentrations of lignin, dense phenolic chemicals.

The 3D Medial Axis (3DMA) codes developed by Lindquist et al[10] were The 3D Medial Axis (3DMA) codes developed by Lindquist et al[10] were used for the segmentation and analysis. These and other codes have been applied for years to the analysis of tomographic data of geological samples[1,3,10] and can be directly applied to the study of any porous or two-element media. All post-rendering analysis of the data was performed using the tools available in the 3DMA code. Smoothing of the

image by anisotropic diffusion was applied to the reconstructed data[13] followed by straightforward global thresholding of the data based on the image intensity histograms generated from the enhanced slice data.

A 3D Medial Axis analysis was performed on the segmented volume for each wood sample. The details of this algorithm are discussed elsewhere[14,10]. Calculations of volume porosity and the interconnectivity of the pore space for each sample were performed to estimate the damage caused by the fungus. Porosity is calculated from the percentage of total voxels found to be pore. It was expected that the porosity would increase with exposure time to the fungus. Adjoining voxels that are identified as pore constitute one disconnected part of the total pore volume. The number of discrete pores and the percent volume they cover gives information about pore connectivity, making 3DMA an ideal tool for geological fluid flow problems for which the code was initially intended. More of the pore space is connected in sound wood, but in fungal degraded wood the wall structure is broken down over time. We hypothesized that connectivity could be used as an indicator of fungal deterioration. Finally, the burn number distribution found in the 3DMA analysis is an indicator of the average thickness of the pore in each sample; large burn numbers represent pore space furthest from a wood interface. Thus, a table of the number of voxels identified at a certain number k, proportional to the radial distance of voxel from a wood interface, gives another measure of the degree of breakdown of the cell wall exposed to fungus.

4. RESULTS AND DISCUSSION

In these and other tomographic studies of wood[7], density differences were observed in the reconstructed tomography slices, reflecting differences in chemical composition of structures within the wood. Control and fungal-exposed wood exhibited variations in density within the wood cell walls. A representative raster scan of the raw slice data of control wood is given in Figure 3, with the high density structures in black and the low density structures in white. The lowest density materials in white are air and fungal structures. Tracheid cell walls are black or gray, reflecting the differences in the primary, secondary and tertiary wall layers. Ray cells and middle lamella are black. Resolution of the images was approximately 5 microns.

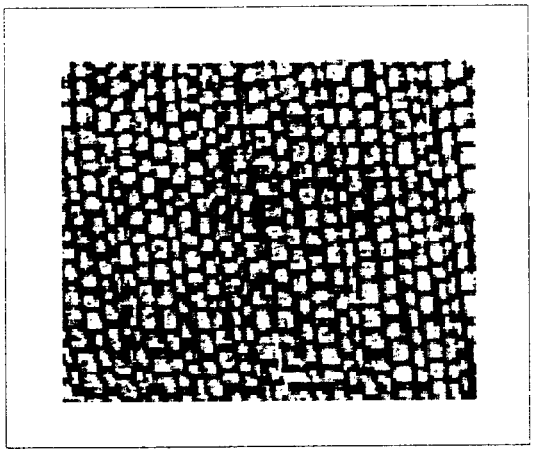

Figure 3. Raster scan of the raw slice

Tracheid cell walls of control wood are connected with no breaks. During incipient decay by the potent brown-rot fungus, *G. trabeum*, a rapid deterioration of the wall occurs. The fungus penetrates wood through natural openings (pits) or by eroding tracheid walls, leaving breaks and holes in the walls. Brown-rot fungi such as *G. trabeum* cause a rapid drop in wood strength properties that is reportedly due to a non-enzymatic depolymerization of structural cellulose[5]. The fungi degrade the cellulose without first removing the lignin, leaving a brown (hence the name brown-rot) residue of partially demethylated lignin. How the rapid change occurs in tracheid walls is an important biochemical question as strength loss can be measured before weight loss of the wood and only 1 percent weight loss of wood can result in a 50 percent loss in wood strength. In this current study, some cell wall breaks were observed in the 4-day experiment.

Erosion of walls typically occurs without visible changes. In reconstructed slices of fungal exposed wood, cell wall structures did not appear quite as dense as those of controls, indicating chemical changes caused by the fungus.

The reconstructed data was segmented and smoothed by the 3DMA codes. An example of the reconstructed slice of control wood in Figure 3, after smoothing and segmentation, is shown in Figure 4. The pixels identified as wood cell walls are colored black whereas those identified as lumen or pore are white. Wood data is particularly difficult to segment because of the thin wall structure (order of 10 microns or less) and the low x-ray absorption of lignocellulose.

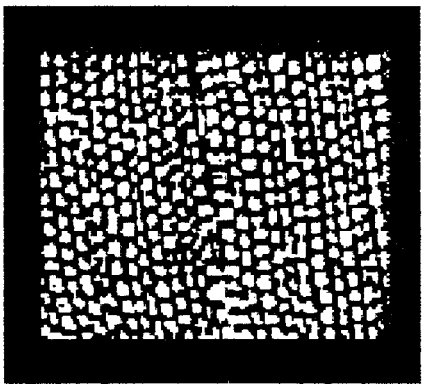

Figure 4. Smoothed and segmented slice

A tabulation of the results from the 3DMA analysis of the segmented volumes for the 4-day experiment is given in Table 1. The total number of voxels in the analyzed volume was over 3 million for every sample. The data supports our hypothesis that samples exposed to the fungus for a longer period of time exhibited a slightly higher percentage of pore space from wall breakdown. The 68-hour had a higher total porosity than the control, 24-hour and 42-hour specimens, but was also higher in porosity than the 92 hour. This could be due to random variability in pore size of specimen, indicating the need for a lager number of samples per scan time.

Table 1. Calculated Porosity

Sample No.	Hours of Exposure	No. of Pore Voxels	Total No. of Voxels	Percent Porosity
1	0	1714608	3640761	47 %
2	24	1724160	3640761	47.3 %
3	42	1901825	3640761	52.2 %
4	68	2087878	3640761	57.3 %
5	92	1977769	3640761	54.3 %

A plot of the burn number distribution for these same three data sets reinforces the disconnectivity plots. These were plotted from the data in Table 2. Burn numbers are proportional to the radius of a pore pixel from a solid interface; large burn numbers represent pore space furthest from a wood voxel. Thus, a table of the number of voxels identified at a certain burn number k gives another measure of the degree of breakdown of the lignin exposed to fungus. The samples exposed to fungus have a larger number of voxels at higher burn numbers, showing an increase in the average pore thickness.

Table 2. Burn Number Distribution

Burn Number	N(k)				
k	Sample 1 Control	Sample 2 24h	Sample 3 42h	Sample 4 68h	Sample5 92h
0	1.670 e+6	1.65 e+6	1.489 e+6	1.405e+6	1.516e+6
1	1.358 e+6	1.374 e+6	1.449 e+6	1.493e+6	1.538e+6
2	343555	338093	429807	547509	426357
3	12570	11955	22676	47040	13374
4	24	30	197	360	80
5		3	1	0	0

Connectivity plots for three samples, the control, after 24 and 68 hours of exposure are shown in Figure 5. Most of the volume for each is connected. One disconnected or discrete pore covers over 40% in each case. The percent volume covered by one pore is the least for the control and the greatest for the sample exposed for 68 hours, as expected. As more of the lignin breaks down, a greater amount of pore voxels become interconnected. This trend is also evident in the plot as the peak number of disconnected pore segments decreases with increasing exposure to the fungus.

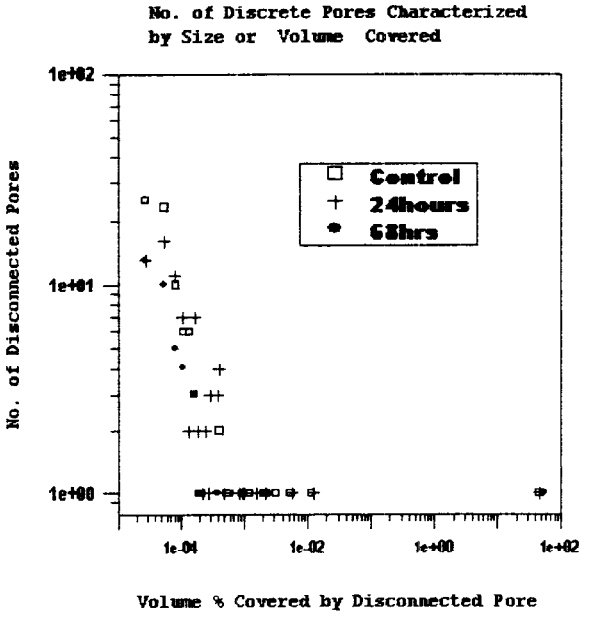

Figure 5. Disconnectivity Curves

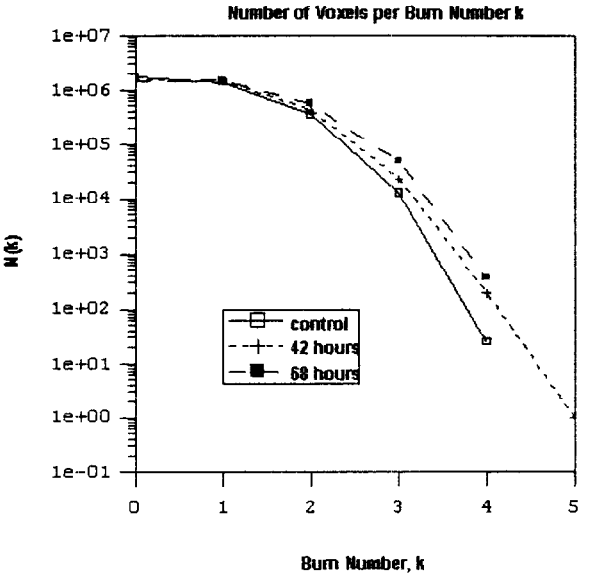

Figure 6. Burn Number Distribution

CONCLUSIONS

This study has demonstrated the feasibility of using gray scale images of tomographic data and porosity and connectivity codes operated on segmented image volumes to characterize the microscale breakdown of wood cell walls by fungi. Future enhancements that will aid in this work include the incorporation of a narrow bandpass Si 111 pair monochromator and a larger number of wood specimens.

ACKNOWLEDGEMENTS

The X-ray Computed Microtomography instrument was funded in part by DOE grant No. DE-AC02-76CH00016, Office of Energy Research. Research on wood degradation was funded in part from USDA Competitive Grant 94-37103-1016 (Illman) and funds from the USDA-FS Forest Products Laboratory.

REFERENCES

1. Coles, M.E., SPE, Hazlett, R.D., Muegge, E.L., Jones, K.W., Andrews, B., Dowd, B., Siddons, P., and Peskin, A., Spanne, P.,Soll, W.E. "Developments in Synchrotron X-Ray Microtomography with Applications to Flow in Porous Media," *Journal of the Society of Petroleum Engineers*, August 1998.
2. Dowd, B.A., Andrews, A.B., Marr, R.B., Siddons, D.P., Jones, K.W., Peskin, A.M., "Advances In X-Ray Computed Microtomography at the NSLS", invited paper, presented at the 47th Annual Denver X-Ray Conference, Colorado Springs, CO, August 3-7, 1998 (BNL-65832) and accepted for publication in *Advances in X-ray Analysis*, **Vol. 42**, May 1999.
3. Ferreol, B. and Rothman, D.H., "Lattice-Boltzmann Simulations of Flow Through Fountainebleau Sandstone," *Transport in Porous Media* **20**, Nos. 1 & 2, 3, 1995.
4. Herman, G.T., *Image Reconstruction From Projections*, Academic Press, 1980.
5. Highley, T.L., C.A. Clausen, S.C. Croan, F. Green III, B.L. Illman, and J.A. Micales. Research on Biodeterioration of Wood, 1987-1992. USDA/FS Forest Products Laboratory Research Paper, FPL-RP-529, 1994.
6. Illman, B.L., Oxidative Degradation of Wood by Brown-rot Fungi. IN: Active Oxygen/Oxidative Stress and Plant Metabolism. Current Topics in Plant Physiology, vol. 6. E.J. Pell, K.L. Steffen and J.C. Shannon, Eds. American Society of Plant Physiologists, Rockville, MD, pp. 97-106, 1992.
7. Illman, B.L. and Dowd, B.A., "Synchrotron Applications in Forestry and Forest Products", *Synchrotron Radiation News*, **Vol. 10, No. 1**, (1997). (Cover)
8. Illman, B.L. and S. Bajt, Nondestructive elemental analysis of wood biodeterioration using electron paramagnetic resonance and synchrotron x-ray fluorescence. International Biodeter. and Biodegrad. 39(2-3): 235-242, 1997.
9. Kak, A.,C., Slaney, M., *Principles of computerized tomographic imaging*, New York : IEEE Press, 1988.
10. Lindquist, W.B., Lee, S-M., Coker, D.A., Jones, K.W., and Spanne, P., "Medial Axis Analysis of Void Structure in Three Dimensional Tomographic Images of Porous Media", *Journal of Geophysical Research B,* **Vol. 101, No.B4** 8297-8310, 1996.
11. Marr, R.B., "Fast Filtered Back-Transform Reconstruction Algorithm for Generalized Fourier Data", *Soc. Of Magnetic Resonance in Med.,* 6th Annual Meeting, 1987.
12. O'Sullivan, J.D., "A Fast Sinc Function Gridding Algorithm for Fourier Inversion in Computer Tomography", *IEEE Transactions on Medical Imaging* 1985.
13. Perona, P., Shiota, T., and Makik, J., "Anisotropic Diffusion", *Geometry Driven Diffusion in Computer Vision*, B.M. ter Haar Romany, ed., pp. 73-92, Kluwer Academic Pub., Boston, 1994.
14. Sirjani, A., and Cross, G.,R., *Pattern Recognition Letters*, **12**, 149-154, 1991.